

# Modelling for the micro-interactions of grit-workpiece in ultrasonic vibration grinding of fused silica glass

Cheng Huang<sup>1,#</sup>, Yupeng Xiong<sup>1</sup>, Yifan Dai<sup>1</sup>, Silin Guo<sup>1</sup>, Hao Hu<sup>1</sup>, and Shanyong Chen<sup>1</sup>

<sup>1</sup> Laboratory of Science and Technology on Integrated Logistics Support, College of Intelligence Science and Technology, National University of Defense Technology, Changsha, Hunan 410073, P.R of China  
# Corresponding Author / Email: hithuangcheng@163.com, TEL: +86-13187089709

KEYWORDS: Ultrasonic vibration side grinding, Micro-interaction effects, Stochastic distribution of grits, Cutting forces

*The cutting force in ultrasonic vibration side grinding (UVSG) of brittle materials is of significance for the machined quality. However, the micro-interaction mechanism between abrasive grits and workpiece remains a significant issue in terms of the research on cutting forces in the brittle material grinding due to the stochastic distribution nature of the grits. Meanwhile, these micro-interactions are further affected by ultrasonic vibration in UVSG process. Considering these issues, this paper aims at modeling the cutting force affected by the stochastically distributed grits and ultrasonic vibration to reveal the multi-scale grinding mechanics in UVSG of fused silica glass. Through modeling the stochastic grinding wheel surface and analyzing the kinematics of multi-grits, the unified motion trajectory and the instantaneous chip thickness in UVSG were enabled to derived to determine the different grit-workpiece interaction stages. With consideration of the ultrasonic vibration effects on the micro-interactions, a novel theoretical cutting force model was developed based on the analysis of force generated at three interaction stages, i.e., rubbing, plowing, and cutting stages. The numerical simulations of this model could provide the time-domain variation features of cutting forces to evaluate the fluctuations and trends of the cutting forces from multi-scales. Experimental verifications indicated that the cutting force and its fluctuations are within the acceptable error margin. Furthermore, a thorough analysis of force fluctuating situations at different ultrasonic vibration amplitudes was conducted. The analytical results indicated that an increase in ultrasonic vibration amplitude was not only beneficial to restrain the force fluctuation, but helpful to reduce the brittle fracture damages of fused silica glass.*

## 1. Introduction

Fused silica glass has superior properties such as high linear transmission, wide transmission range, high mechanical strength, and low thermal expansion coefficient<sup>[1]</sup>. It covers a broad range of applications in related industries in recent years, especially in high-power laser systems<sup>[2]</sup>. All these advanced components demand high precision and low damages in manufacturing processes. However, conventional machining methods for fused silica glass easily induce surface/subsurface damage due to its high hardness, brittleness, and low fracture toughness which affects the component performances<sup>[3]</sup>. Therefore, it is challenging to achieve the desired accuracy, high efficiency, and cost-effective processing for Fused silica glass.

Ultrasonic vibration grinding (UVG) is a novel hybrid machining technology with multiple benefits in terms of reducing grinding force, tools wear, and increasing material removal rate<sup>[4]</sup>. It combines the material removal mechanism of conventional grinding process and ultrasonic machining<sup>[5]</sup>. A special designed hollow-cone diamond wheel is utilized in the process. The diamond grinding wheel vibrates along the axial direction at an amplitude of about 1-10 $\mu$ m and a frequency of about 15-40kHz while it rotates and fed toward the

workpiece. UVG has been recognized as an efficient machining method for hard and brittle materials, including fused silica glass, sapphire, and ceramics<sup>[6]</sup>. To some extent, the problems in fused silica glass manufacturing are resolved by the introduction of ultrasonic machining technology to conventional grinding process. Nowadays perpetual efforts are being made by researchers to explore the full potential of the UVG method for the benefits of suppression manufacturing defects and enhanced machining efficiency.

The magnitude of grinding force is an important output variable during grinding process which affects directly the machined surface/subsurface quality and machining precision of hard and brittle materials<sup>[7, 8]</sup>. Research on theoretical prediction of grinding forces in UVG process is crucial both for a better understanding of the material removal mechanism in UVG, and for exploring the effective processing method to reduce the manufacturing defects<sup>[9]</sup>.

Several significant investigations had been conducted based on the prediction of material removal rate in rotary ultrasonic machining by Pei et al. <sup>[10]</sup>. Following that, Liu et al. <sup>[11]</sup> proposed a mathematical model under the hypothesis that brittle fracture was the primary mechanism of material removal in ultrasonic machining for brittle materials and the relationship between machining parameters and

grinding force was discussed. In addition, Xiao et al. [12] considered the critical cutting depth of ductile-to-brittle transition for brittle materials and the average cutting depth in ductile and brittle regions respectively to develop the grinding force models in UVG. Sun et al. [13] developed a grinding force prediction model for UVG of glass material, and the grinding force was separated into three primary force components in the model. Similar research works on grinding force prediction in UVG were also reported in other literatures [14, 15].

However, only the average cutting depth and average chip thickness were considered in most models. The influence of the actual protrusion heights of grains on the grinding force was usually ignored. Feng et al. [16] proposed three kinds of tool-workpiece separation criterion based on kinematic analysis, and firstly predicted the cutting forces in feed, cutting and axial directions during all types of vibration assisted milling. But this reported model is not suitable for grinding force prediction in the machining process with the grinding wheel, in which the nonuniform distribution of abrasive grits on the wheel would lead to different contact situations between the cutting tips and workpiece. Therefore, a theoretical grinding force prediction model has been established in UVG for fused silica glass with the consideration of both the nonuniform distribution of wheel morphologies and energy perspective in this work. Meanwhile, the predicted model was vitrified by grinding experiments.

## 2. Development of grinding force model

### 2.1 Measurement and modelling of grinding wheel surface morphology

As the nonuniform distribution of the protrusion height of individual grits on the wheel surface would exert a great influence on the cutting force in UVG process. Therefore, the measurement and modelling of grinding wheel surface morphology are conducted to obtain the data of the protrusion height of these grits in this work.

Table 1 Technical data of the grinding wheel used in modelling.

Abrasive	Diamond
Bond type	Metal-bond
Outer diameter $D_o$ (mm)	2
Interior diameter $D_i$ (mm)	1
Abrasive mesh size $S_a$ ( $\mu$ m)	58
Abrasive concentration $C_a$	100
Volume concentration $V_g$	25%

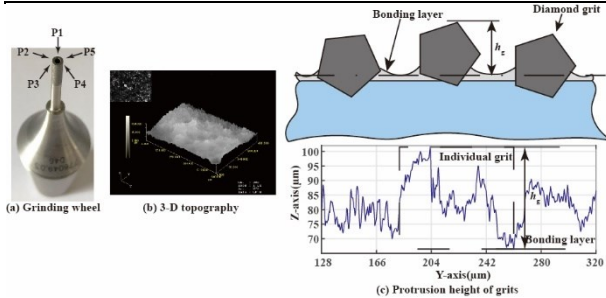


Fig. 1 Illustrations of measuring process for grinding wheel end-face topology.

As shown in Table 1 and Fig. 1(a), a diamond metal-bonded hollow

grinding wheel was used in modelling of the wheel surface morphology. The wheel end-face was marked with 5 positions (P1-P5) for repeated measurements. A confocal laser scanning microscope (OLYMPUS OLS 3000) was employed to acquire the three-dimension topography of the grinding wheel surface, as shown in Fig. 1(b). The surface profile of the wheel surface is obtained by extracting the cross section in the axial direction. The individual grit with the bonding layer could be considered as a profile element. Then the height of these profile elements can be considered as the grain protrusion height  $h_g$ , which is measured from the bonding layer (the lowest position in the profile element) to the grit top (exceeding the mesh size of grit) as shown in Fig. 1(c) [17]. At each marked sampling position, the axial run-out of wheel is considered constant for all scanning grains.

The protrusion height of grits could be assumed to follow the normal distribution law [17, 18]. Fig. 2(a) presents the distribution frequency of the grit protrusion height  $h_g$  at marked positions. Obviously, the distribution of  $h_g$  at each position on the wheel surface approach to the normal distribution law. Therefore, the frequency histogram for  $h_g$  at all sampling positions is presented in Fig. 2(b).

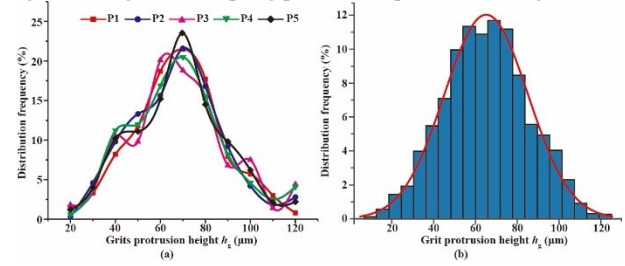


Fig. 2. Normal distribution plots of protrusion height of abrasive grain  $h_g$ . (a) At each marked position, (b) At total five positions.

To verify the assumption, the methods of Kolmogorov-Smirnov test (K-S test) is performed to evaluate the normality degree of the grits protrusion height [19]. Indeed, the results (listed in Table 2) show that the significance value of K-S test is much larger than 0.05, which suggests that the data of  $h_g$  is in normal distribution. The statistical data of  $h_g$  are listed in Table 2.

Table 2 Kolmogorov-Smirnov test results and statistical data.

Sample size	Mean value	Standard deviation value	Sig.
$N$	$h_{mean}$ ( $\mu$ m)	( $\mu$ m)	
512×512	64.20	20.36	0.194

Since the measured data of  $h_g$  coincides with normal distribution law, the modeled surface topology of the grinding wheel surface can be reconstructed by a  $m \times n$  matrix, as expressed in Eq. (1)

$$H = \left( h_{g,(i,j)} \right)_{m \times n} \quad (1)$$

where  $h_{g,(i,j)}$  stands for  $h_g$  in the  $i$ th row and the  $j$ th column.

### 2.2 Kinematical analysis of the single diamond grit in UVG

The UVG process can be considered as the combination of the grinding and axial ultrasonic vibration of all grits on the grinding wheel. The motion of the single grit on the wheel consists of spindle rotation, horizontal feed motion and axial ultrasonic vibration in the coordinate system Oxyz. The initial phase of the ultrasonic vibration is assumed 0 at the beginning of grinding process. Therefore, the trajectory equation of the single grit in UVG can be expressed as Eq. (2):

$$S(t) = \begin{cases} S_x(t) \\ S_y(t) \\ S_z(t) \end{cases} = \begin{cases} 0.5D_o \cos \omega t + v_f t \\ 0.5D_o \sin \omega t \\ A \sin 2\pi f t \end{cases} \quad (2)$$

where  $D_o$  is the outer diameter of the grinding wheel, mm;  $\omega = \pi n/30$  is the angular velocity of the grits, rad/s,  $n$  is the spindle rotation speed, rpm;  $v_f$  is the feed rate, mm/s;  $t$  is the cutting time, s;  $A$  is the ultrasonic vibration amplitude,  $\mu\text{m}$ ;  $f$  is the vibration frequency, Hz. Moreover, the velocity of the single diamond grit ( $v(t)$ ) in the coordinate system can be obtained by differentiating the Eq. (2).

### 2.3 Material removal rate modelling in UVG

The grinding experimental results present that the axial grinding force  $F_c$  is the main component among of three measured components of grinding force. Moreover, the impact-separation effect from ultrasonic vibration is mainly reflected in the axial direction.

During each ultrasonic vibration period, the grits are in noncontinuous contact with the workpiece surface for a certain period of time, as shown in Fig. 3. In the effective material removal process, the effective cutting time is  $\Delta t$ , and the maximum penetration depth is  $\delta_m$ . From the kinematic trajectory equation of the single grit (Eq. (2)), the effective cutting time  $\Delta t$  can be expressed as:

$$\Delta t = 2(t_2 - t_1) = \frac{1}{\pi f} \left[ \frac{\pi}{2} - \arcsin \left( 1 - \frac{\delta_m}{A} \right) \right] \approx \frac{\delta_m}{2Af} \quad (3)$$

where,  $\delta_m$  is the maximum penetration depth between the grits and workpiece surface, mm.

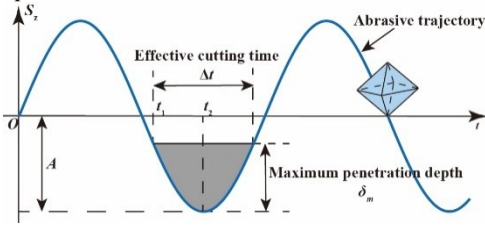


Fig. 3. Schematic illustration of effective cutting time in a single vibration period.

Then the effective cutting length of single grit  $l_s$  in the effective cutting time  $\Delta t$  can be determined by the velocity of the abrasive grit  $v(t)$  and the effective cutting time  $\Delta t$ :

$$l_s = \int_{t_1}^{t_2} v(t) dt \approx \frac{\pi n (D_o + D_i)}{120} \Delta t \quad (4)$$

In UVG process of fused silica glass, as shown in Fig. 4(a), the grit penetration depth increases from  $\delta=0$  to  $\delta=\delta_m$  and then declines to  $\delta=0$  during a single effective cutting time, as the grit goes through the effective cutting length  $l_s$  on the workpiece. In Fig. 4(b), half of the brittle fracture region is simplified as a tetrahedron HABC, in which the straight-line HC and HB represent the lateral cracks induced as the penetration depth reaching  $\delta_m$ . Therefore, the theoretical material removal volume  $V$  can be expressed as:  $V=2V_{HABC}=C_L C_h l_s / 3$ . The lateral crack characteristic dimension of the length  $C_L$  and the depth  $C_h$  can be calculated by<sup>[20]</sup>:

$$\begin{cases} C_L = C_2 \tan^{-5/12} \theta \left[ \frac{E^{3/4}}{H_v K_{IC} (1-\nu^2)^{1/2}} \right]^{1/2} F_m^{5/8} \\ C_h = C_2 \tan^{-1/3} \theta \frac{E^{1/2}}{H_v} F_m^{1/2} \end{cases} \quad (5)$$

where  $C_2$  is a dimensionless constant depending on the indenter system, and  $C_2=0.226$ ;  $\theta$  is the semi-angle between two opposite edge of the grits;  $K_{IC}$  is the fracture toughness of workpiece materials;  $H_v$  is the Vickers hardness;  $\nu$  is the Poisson's ratio;  $E$  is the elastic modulus; and  $F_m$  is the maximum contact force for the single grit, N.

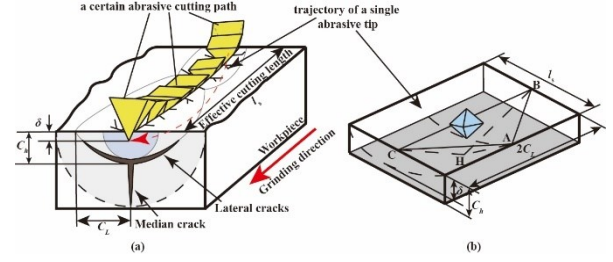


Fig. 4. Schematic illustration of material removal process in brittle fracture mode in UVG. (a) Microscopic view of grinding process, (b) The volume of brittle fracture material removal by single grit.

Thus, the theoretical material removal rate for single grit  $M_T$  is defined as:

$$M_T = V f = C_L C_h l_s f / 3 \quad (6)$$

And the material removal rate for all the effective grits  $M$  can be obtained by the effective grits number  $N_e$  and theoretical material removal rate  $M_T$ :

$$M = N_e M_T = C_0 \frac{C_a^{2/3} A_0}{3S_a^2} C_L C_h l_s f \quad (7)$$

where  $C_0$  is a dimensionless constant related to the density of abrasive material, for diamond,  $C_0=0.03$ ;  $C_a$  is the grit concentration, and  $S_a$  is the grit size;  $A_0$  is the contact area of the grinding wheel surface. Additionally, the mean values of abrasive size ( $S_a$ ), is approximate to the mean values of the protrusion height of abrasive grits, ( $h_{mean}$ ).

Meanwhile, the actual material removal rate  $M_a$  can be presented as:  $M_a = A_0 \cdot v_f$ . Then the correction coefficient  $K$  will be introduced to correct the different between  $M_a$  and  $M$ , which could be presented as:

$$M_a = K \cdot M \quad (8)$$

where  $K$  is a proportionality coefficient, and it is assumed to be constant for a certain workpiece-tool system.

### 2.4 Grinding force prediction model in UVG

Since the ultrasonic vibration superposes along the axial direction, only the effect of impact force is taken account in the grinding force model. For the effective grits the maximum impact force  $F_n$  could be derived by  $F_m$ <sup>[21]</sup>:

$$F_n = N_e \cdot F_m = N_e \zeta \delta_m^2 \tan \theta H_v / 2 \quad (9)$$

The grits could be regarded as an ideal rigid body with incompressibility and the effective cutting time  $\Delta t$  is very short from Eq. (3) ( $\delta_m \ll Af$ ), the impulse  $I$  in term of the impact force over the time  $F(t)$  during one ultrasonic vibration period can be approximated to the impulse in term of the maximum impact force  $F_m$ . Thus, the impulse  $I$  can be described as:

$$I = \int_T F(t) dt \approx F_n \Delta t \quad (10)$$

The impulse  $I$  also can be expressed in term of the grinding force  $F_c$  during one ultrasonic vibration period:  $I = F_c / f$ .

Due to these impulse values  $I$  are actually on behalf of the same physical process, so there is:

$$F_c = F_n \cdot \Delta t \cdot f = N_e F_m \Delta t f \quad (11)$$

By substituting Eq. (3), (4), (5), and (7) into Eq. (8), the maximum penetration depth  $\delta_m$  can be expressed as:

$$\delta_m = \left[ \frac{C_3}{K} \cdot \frac{v_f A K_{IC}^{1/2} (1-v^2)^{1/4} H_v^{3/8} \cot^{3/8} \theta}{n C_a^{2/3} R E^{7/8} \zeta^{9/8}} h_{mean}^2 \right]^{4/13} \quad (12)$$

where  $C_3 = 180 \cdot (C_0 C_2^2 \pi)^{-1}$ .

According to the section 2.1, the protrusion height of the grits  $h_g$  follows the normal distribution. Therefore, the maximum penetration depth  $\delta_m$  also follows normal distribution law. By substituting the reconstruction wheel surface model from Eq. (1) into Eq. (12), and rewritten Eq. (11), the grinding force  $F_c$  could be presented as:

$$F_c = \sum_{i,j=1}^{N_g} f \cdot F_m^{(i,j)} (\delta_{m(i,j)}) \Delta t \quad (13)$$

### 3. Verification of the proposed grinding force model

In order to validate the grinding force prediction model developed in this study, the validation experiments with varied grinding and ultrasonic parameters are performed.

The axial ultrasonic vibration grinding experiments were conducted on a five-axis precision ultrasonic machine center (DMG Ultrasonic 70-5 Linear). Fig. 5 shows the entire grinding experiment setup. The grinding tool is fixed on the ultrasonic spindle system and oscillates along the axial direction of the spindle with the resonance frequency of machine system at 30kHz and the maximum amplitude is 10μm for the selected grinding tool.

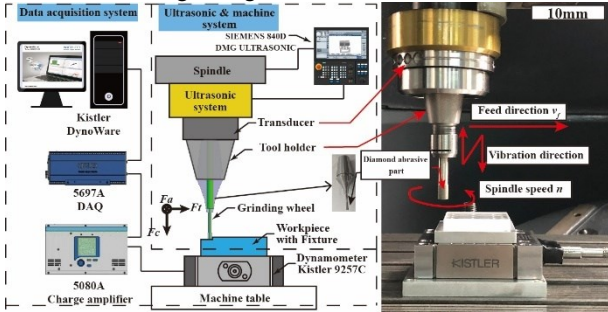


Fig. 5. Schematic of the UVG experiment setup

The diamond metal-bonded tools are provided by SCHOTT Diamond Tools Corp. (Stadtdoldendorf, Germany). The detailed technical data of the diamond tools used in the experiments are listed in Table 1. The fused silica glass specimen with the dimension of 30mm (length)×30mm (width)×8mm (height) was used in the experiments, the material properties are shown in Table 3. To reduce influences from previous defects and scratches, the polishing operation was conducted on the specimen surface before experiments.

Table 3 Material properties of fused silica glass.

Property	Unit	Value
Density $\rho$	g/cm <sup>3</sup>	2.530
Elastic modulus $E$	GPa	82
Poisson's ratio $\nu$	-	0.28
Fracture toughness $K_{IC}$	MPa·m <sup>1/2</sup>	0.82
Vickers hardness $H_v$	GPa	7.2

The grinding parameters of verification experiments are given in the Table 4. The grinding force were measured by a Kistler 9257C

dynamometer, whose sampling frequency was 10kHz, as shown in Fig. 5.

Table 4 Experiments design for verifying the prediction model.

Spindle speed $n$ (rpm)	Feed rate $v_f$ (mm/min)	Cutting depth $a_p$ (μm)	Amplitude $A$ (μm)
6000,8000,10000, 12000,14000	60	20	10
10000	40,50,60,70,80	20	10
10000	60	10,15,20,25,30	10
10000	60	20	0,2,4,6,8,10

The comparison between average experimental and predicted cutting force results has been shown in Fig. 6. It can be seen from Fig. 6(d) that the average grinding force is 15.45N for conventional grinding ( $A=0$ ). As the vibration amplitude is 2μm, the average grinding force is 12.12N for UVG. The average grinding forces decrease by 21.6% when the ultrasonic vibration is exerted on the grinding tool and the average grinding forces keep declining trend when vibration amplitude increases.

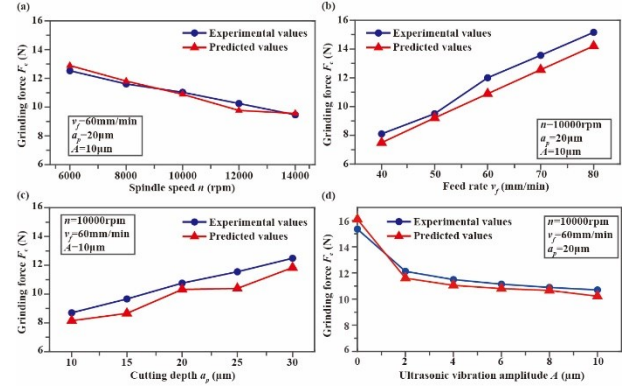


Fig. 6. Experimental and predicted average grinding force values comparison

It is found that the corresponding prediction values for the cutting force are consistent with the experimental results in given parameters ranges. Meanwhile, the average values of relative error for each varied parameter have been listed in Table 6. The maximum average relative error between predicted and experimental results is 10.37%, and the total relative average error is 4.94%. The proposed model in this work shows approximate or better predicted ability comparing with some existing models.

### 4. Conclusion

In this paper, a theoretical model was proposed for predicting grinding force in axial ultrasonic vibration grinding of fused silica glass. As an innovation, this prediction model introduced a novel method to consider the effect of nonuniform distribution of protrusion height of grits on the grinding force. The validation experiments were conducted to demonstrate the effectiveness of this prediction model.

### ACKNOWLEDGEMENT

This work was supported by the National Natural Science

Foundation of China (Grant No. 52305520).

## REFERENCES

1. Moore, L. A. and Smith, C. M., "Fused Silica as an Optical Material [Invited]," *Opt. Mater. Express*, Vol. 12, No. 8, pp. 3043-3059, 2022.
2. Wei, W., Yao, P., Wang, J. et al., "Elastic Stress Field Model and Micro-Crack Evolution for Isotropic Brittle Materials During Single Grit Scratching," *Ceram. Int.*, Vol. 43, pp. 10726-10736, 2017.
3. Goel, S., Luo, X., Agrawal, A. et al., "Diamond Machining of Silicon: A Review of Advances in Molecular Dynamics Simulation," *Int. J. Mach. Tools Manuf.*, Vol. 88, pp. 131-164, 2015.
4. Yang, Z., Zhu, L., Zhang, G. et al., "Review of Ultrasonic Vibration-Assisted Machining in Advanced Materials," *Int. J. Mach. Tools Manuf.*, Vol. 156, p. 103594, 2020.
5. Pei, Z. J., Ferreira, P. M., Kapoor, S. G. et al., "Rotary Ultrasonic Machining for Face Milling of Ceramics," *Int. J. Mach. Tools Manuf.*, Vol. 35, No. 7, pp. 1033-1046, 1995.
6. Singh, R. P. and Singhal, S., "Rotary Ultrasonic Machining: A Review," *Mater. Manuf. Process.*, Vol. 31, No. 14, pp. 1795-1824, 2016.
7. Pereverzev, P. P. and Pimenov, D. Y., "A Grinding Force Model Allowing for Dulling of Abrasive Wheel Cutting Grains in Plunge Cylindrical Grinding," *J. Frict. Wear.*, Vol. 37, No. 1, pp. 60-65, 2016.
8. Zhang, J., Li, H., Zhang, M. et al., "Study on Force Modeling Considering Size Effect in Ultrasonic-Assisted Micro-End Grinding of Silica Glass and  $\text{Al}_2\text{O}_3$  Ceramic," *Int. J. Adv. Manuf. Technol.*, Vol. 89, No. 1-4, pp. 1173-1192, 2017.
9. Baraheni, M. and Amini, S., "Predicting Subsurface Damage in Silicon Nitride Ceramics Subjected to Rotary Ultrasonic Assisted Face Grinding," *Ceram. Int.*, Vol. 45, No. 8, pp. 10086-10096, 2019.
10. Pei, Z. J., Prabhakar, D., Ferreira, P. M. et al., "A Mechanistic Approach to the Prediction of Material Removal Rates in Rotary Ultrasonic Machining," *J. Manuf. Sci. Eng.*, Vol. 117, No. 2, pp. 142-151, 1995.
11. Liu, D., Cong, W. L., Pei, Z. J. et al., "A Cutting Force Model for Rotary Ultrasonic Machining of Brittle Materials," *Int. J. Mach. Tools Manuf.*, Vol. 52, No. 1, pp. 77-84, 2012.
12. Xiao, X., Zheng, K., Liao, W. et al., "Study on Cutting Force Model in Ultrasonic Vibration Assisted Side Grinding of Zirconia Ceramics," *Int. J. Mach. Tools Manuf.*, Vol. 104, pp. 58-67, 2016.
13. Sun, G. Y., Zhao, L. L., Zhao, Q. L. et al., "Improved Force Prediction Model for Grinding Zerodur Based on the Comprehensive Material Removal Mechanism," *Appl. Opt.*, Vol. 57, No. 14, pp. 3704-3713, 2018.
14. Amin, M., Yuan, S., Khan, M. Z. et al., "Development of a Generalized Cutting Force Prediction Model for Carbon Fiber Reinforced Polymers Based on Rotary Ultrasonic Face Milling," *Int. J. Adv. Manuf. Technol.*, Vol. 93, No. 5-8, pp. 2655-2666, 2017.
15. Baraheni, M. and Amini, S., "Mathematical Model to Predict Cutting Force in Rotary Ultrasonic Assisted End Grinding of  $\text{Si}_3\text{N}_4$  Considering Both Ductile and Brittle Deformation," *Measurement*, Vol. 156, p. 107586, 2020.
16. Feng, Y., Hsu, F.-C., Lu, Y.-T. et al., "Force Prediction in Ultrasonic Vibration-Assisted Milling," *Mach. Sci. Technol.*, Vol. 25, No. 2, pp. 307-330, 2020.
17. Dai, C. W., Yin, Z., Ding, W. F. et al., "Grinding Force and Energy Modeling of Textured Monolayer CBN Wheels Considering Undeformed Chip Thickness Nonuniformity," *Int. J. Mech. Sci.*, Vol. 157, pp. 221-230, 2019.
18. Zhou, X. and Xi, F., "Modeling and Predicting Surface Roughness of the Grinding Process," *Int. J. Mach. Tools Manuf.*, Vol. 42, pp. 969-977, 2002.
19. Ding, W. F., Dai, C. W., Yu, T. Y. et al., "Grinding Performance of Textured Monolayer CBN Wheels: Undeformed Chip Thickness Nonuniformity Modeling and Ground Surface Topography Prediction," *Int. J. Mach. Tools Manuf.*, Vol. 122, pp. 52-66, 2017.
20. Lawn, B. R., Evans, A. G., and Marshall, D. B., "Elastic/Plastic Indentation Damage in Ceramics: The Median/Radial Crack System," *Journal of the American Ceramic Society*, Vol. 65, No. 11, pp. 561-566, 1982.
21. Wang, J., Feng, P., Zhang, J. et al., "Investigations on the Critical Feed Rate Guaranteeing the Effectiveness of Rotary Ultrasonic Machining," *Ultrasonics*, Vol. 74, pp. 81-88, 2017.